

This is the author-created version of the following work:

**Rowe, Cassandra, Wurster, Christopher M., Zwart, Costijn, Brand, Michael, Hutley, Lindsay B., Levchenko, Vladimir, and Bird, Michael I. (2021) *Vegetation over the last glacial maximum at Girraween Lagoon, monsoonal northern Australia*. *Quaternary Research*, 102 pp. 39-52.**

Access to this file is available from:

<https://researchonline.jcu.edu.au/65697/>

© University of Washington. Published by Cambridge University Press, 2020

Please refer to the original source for the final version of this work:

<https://doi.org/10.1017/qua.2020.50>

1 **Vegetation over the last glacial maximum at Girraween Lagoon, monsoonal northern**  
2 **Australia**

3 Cassandra Rowe<sup>a\*</sup>, Christopher M. Wurster<sup>a</sup>, Costijn Zwart<sup>a</sup>, Michael Brand<sup>a</sup>, Lindsay  
4 Hutley<sup>b</sup>, Vladimir Levchenko<sup>c</sup>, Michael I. Bird<sup>a</sup>

5 <sup>a</sup>College of Science and Engineering, ARC Centre of Excellence of Australian Biodiversity  
6 and Heritage and Centre for Tropical Environmental and Sustainability Science, James Cook  
7 University, Cairns, QLD 4870, Australia

8 <sup>b</sup>Research Institute for the Environment and Livelihoods, Charles Darwin University,  
9 Darwin, Northern Territory 0909, Australia

10 <sup>c</sup>Australian Nuclear Science and Technology Organization, Locked Bag 2001, Kirrawee DC  
11 NSW 2232, Australia

12 \*Corresponding author at: College of Science and Engineering, ARC Centre of Excellence of  
13 Australian Biodiversity and Heritage and Centre for Tropical Environmental and  
14 Sustainability Science, Cairns Campus, 14–88 McGregor Road, James Cook University,  
15 Cairns, QLD 4870, Australia.

16 E-mail address: [cassandra.rowe@jcu.edu.au](mailto:cassandra.rowe@jcu.edu.au) (C. Rowe)

17

18 RECEIVED JANUARY 13, 2020; ACCEPTED MAY 05, 2020

19

20

21

## 22 **Abstract**

23 Northern Australia is a region where limited information exists on environments at the last  
24 glacial maximum (LGM). Girraween Lagoon is located on the central northern coast of  
25 Australia and is a site representative of regional tropical savanna woodlands. Girraween  
26 Lagoon remained a perennial waterbody throughout the LGM, and as a result retains a  
27 complete proxy record of last-glacial climate, vegetation and fire. This study combines  
28 independent palynological and geochemical analyses to demonstrate a dramatic reduction in  
29 both tree cover and woody richness, and an expansion of grassland, relative to current  
30 vegetation at the site. The process of tree decline was primarily controlled by the cool-dry  
31 glacial climate and CO<sub>2</sub> effects, though more localised site characteristics restricted wetland-  
32 associated vegetation. Fire processes played less of a role in determining vegetation than  
33 during the Holocene and modern day, with reduced fire activity consistent with significantly  
34 lower biomass available to burn. Girraween Lagoon's unique and detailed palaeoecological  
35 record provides the opportunity to explore and assess modelling studies of vegetation  
36 distribution during the LGM, particularly where a number of different global vegetation  
37 and/or climate simulations are inconsistent for northern Australia, and at a range of  
38 resolutions.

39

## 40 **KEYWORDS**

41 Tropical savanna; Grassland; Tree cover; Pollen; Charcoal; Carbon isotope; Model;  
42 Monsoon; Northern Australia; Last Glacial Maximum.

43

44

45

## 46 INTRODUCTION

47           The last glacial maximum (LGM; centred on 21 ka) was the most recent time when  
48 ice sheets were at their maximum extent and hence sea level was at its lowest (Clark et al.,  
49 2009; Hopcroft and Valdes, 2015). Lowered sea level led to dramatic increases in land area in  
50 some parts of the world. Equally dramatic changes in the distribution of terrestrial biomes  
51 were driven by decreases in temperature, changes in the distribution and amount of  
52 precipitation, and lower atmospheric CO<sub>2</sub> (Ganopolski et al., 1998; Shakun and Carlson,  
53 2010; Alder and Hostetler, 2015; Jiang et al., 2015).

54           Mapping regional changes in palaeogeography and climate at the LGM through the  
55 development of palaeoenvironmental proxy records from around the world is key to  
56 understanding modern patterns of biodiversity (Weigelt et al., 2016; Blonder et al., 2018; Ye  
57 et al., 2019) as well as the timing and trajectory of human dispersal (Gavashelishvili and  
58 Tarkhnishvili, 2016; Vahdati et al., 2019) and adaptation (Williams et al., 2018). The  
59 mapping of biome distributions at the LGM also provides empirical insight into climate at the  
60 LGM and therefore the opportunity to evaluate the reliability of climate and carbon/water  
61 models in reproducing observations from outside the comparatively small range of recent  
62 observed climate variability (Harrison et al., 2015).

63           Computer simulations, now Dynamic Global Vegetation Models (DGVMs), have  
64 long been used to simulate biome distributions in the present (Prentice et al., 1992) and at the  
65 LGM (Harrison and Prentice, 2003). The spatial distribution of vegetation types is driven by  
66 one or more general circulation models (GCMs), more recently incorporating other factors  
67 including plant responses to CO<sub>2</sub> (e.g., Cleator et al., 2019), fire regime (e.g., Calvo and  
68 Prentice., 2015; Scheiter et al., 2015) and herbivore biomass (Zhu et al., 2018). Simulations

69 are tested against observations derived from well-dated proxy records, mostly commonly  
70 palynological investigations (Bartlein et al., 2011; Harrison et al., 2015).

71 The spatial distribution of observations of vegetation at the LGM (here defined as 21  
72  $\pm 2$  ka; Hopcroft and Valdes, 2015) is clearly critical to achieving an observation-informed  
73 representation of biome distribution at the LGM. Observations of sufficient quality for this  
74 purpose are currently weighted heavily toward studies from the higher latitudes, with much  
75 patchier representation of low latitude areas (Bartlein et al., 2011; Cleator et al., 2019). This  
76 in turn means that observations provide no empirical constraints on vegetation for large parts  
77 of the terrestrial biosphere, with those in the southern hemisphere biosphere particularly poor  
78 (Cleator et al., 2019).

79 Northern Australia is one region where there is limited information on vegetation  
80 distribution at the LGM (Pickett et al., 2004), with the only sites in the global database of  
81 Bartlein et al. (2011) located on the northeast coast—a wet, mountainous, tropical forest  
82 covered region that is atypical of the rest of tropical Australia. At the LGM, lowered sea level  
83 (Yokoyama et al., 2019) meant that much of the modern landmass of northern Australia was  
84  $\sim 300$  km inland of the LGM coast (Williams et al., 2018). Currently, the equivalent distance  
85 inland reduces mean annual precipitation from 1700 mm to approximately 1000 mm. This  
86 rainfall gradient inland from the coast, along with potential changes in monsoon strength at  
87 the LGM (Jiang et al., 2015; Denniston et al., 2017; Yan et al., 2018) means northern  
88 Australia is sensitively placed to provide a meaningful test of DGVM skill using LGM  
89 boundary conditions. Recent modelling studies of vegetation distribution during the LGM  
90 using a number of different DGVMs and GCMs, at a range of resolutions, have not converged  
91 on a common result for the northern Australian region, with simulations broadly  
92 characterizable as ranging from grassland through savanna woodland to tropical forest (Calvo

93 and Prentice, 2015; Gavashelishvili and Tarkhnishvili, 2016; Zhu et al., 2018; Lu et al., 2019;  
94 Chen et al., 2019; Dallmeyer et al., 2019).

95 Here we present a detailed palynological investigation of the LGM from Girraween  
96 Lagoon near Darwin, on the central northern coast of Australia. This site is representative of  
97 the lowland tropical savanna-woodlands of northern Australia, at the southern end of the  
98 Indonesian-Australian Summer Monsoon (IASM) region. Scheiter et al. (2015) have  
99 demonstrated that Australian tropical savannas are currently sensitive to both climate change  
100 and fire management. It is the primary purpose of this paper to provide a detailed assessment  
101 of the response of vegetation to LGM environmental conditions at a location representative of  
102 the tropical savannas that currently cover approximately 20% of Australia's landmass.

103

## 104 **STUDY AREA AND METHODS**

### 105 **Study area**

106 Girraween Lagoon is one of a number of lagoons that occur across the Northern  
107 Territory's (NT's) Darwin region (Fig. 1). The site is located within the Howard River sub-  
108 catchment of Darwin Harbour (12.517°S, 131.081°E; 28 km inland from the harbour's  
109 northern shoreline and tidal estuaries 15 km west; Schult, 2004). An extensive overview of  
110 the regional context has been provided by Rowe et al. (2019a) and only a brief description is  
111 given here.

112 The Köppen-Geiger classification (as redefined by Peel et al., 2007) characterises the  
113 northern NT climate as Tropical Savanna (code Aw). A distinctive feature of this region's  
114 climate is strong rainfall seasonality, driven by the annual north-south migrating Intertropical  
115 Convergence Zone (ITCZ) with associated convective activity and extreme weather events

116 such as tropical cyclones. El Niño–Southern Oscillation (ENSO) is currently an important  
117 driver in inter-annual variations in rainfall of the region (Charles et al., 2016). Mean annual  
118 Darwin rainfall is 1731.2 mm, and approximately 95% of this total falls during the wet-season  
119 months (November–April). Darwin experiences uniformly high temperatures; mean monthly  
120 maximum-minimum temperatures are 32.1°C and 23.2°C, respectively. Evaporation is also  
121 high year-round, but exhibits a strong seasonal pattern, ranging from ca. 200 mm per month  
122 during the October wet season build-up to ca.125 mm per month during the middle (June) of  
123 the dry season (Charles et al., 2016; Bureau of Meteorology, 2019, Darwin Airport, station  
124 014015, 1941–2018).

125         Girraween Lagoon is a perennial fresh waterbody, with a surface area of 45 hectares  
126 (ha) and a maximum depth of 5 m. Water drains into the lagoon from a catchment of 917 ha.  
127 The lagoon is immediately underlain by lateritized and heavily weathered sandy to clayey  
128 Cretaceous sediments (30–50 m depth). These sediments are underlain by a Proterozoic  
129 dolomite aquifer. The lagoon originated as sinkhole due to collapse into voids created by  
130 dissolution of this underlying dolomite (McFarlane et al., 1995).

131         Modern catchment vegetation comprises tropical mesic open-forest savanna and/or  
132 savanna woodland (Hutley et al., 2013; Moore et al., 2016). *Eucalyptus tetradonta*, *E.*  
133 *miniata*, and *Corymbia polycarpa* (all Eucalyptae: Myrtaceae) dominate the overstorey.  
134 Other prominent tree species include *Erythrophleum chlorostachys* (Caesalpinioideae:  
135 Fabaceae), *Lophostemon lactifluus* (Lophostemoneae: Myrtaceae) and *Terminalia*  
136 *ferdinandiana* (Combretaceae). In the understorey, *Sorghum* and *Heteropogon* (Poaceae)  
137 species are abundant. Saplings, shrubs (e.g., *Pandanus* [Pandanaeae], *Grevillea* [Proteaceae],  
138 *Calytrix* [Chamelaucieae: Myrtaceae] and broad-leaf herbs (e.g., *Spermacoce* [Rubiaceae],  
139 *Murdannia* [Commelinaceae]), *Flagellaria* [Flagellariaceae]) vary in density and height,  
140 dependent on seasonal rainfall variation and fire history. Variable transitional plant

141 communities occur on approach to the water, including mixed monsoonal and/or riparian  
142 forest associations; see Web and Tracey (1994) for discussion on monsoon-type drier  
143 rainforests, and Brock (1995) for survey results on Darwin remnant mixed species woodland.  
144 *Melaleuca symphyocarpa*, *M. viridiflora* and/or *M. cajuputi* (Melaleuceae: Myrtaceae) along  
145 with Cyperaceae-dominated sedgeland, form a swamp fringe around open water. Aquatic  
146 plants include *Nymphaea hastifolia* and *N. violacea* (Nymphaeaceae) as well as submergents  
147 such as *Najas* (Hydrocharitaceae). Girraween's catchment has burnt  $\leq 6-7$  times since the  
148 year 2000, equating to a fire return interval of 2–3 years, a typical regime of northern NT  
149 savanna (Russell-Smith and Yates, 2007).

150           The Larrakia Nation maintains Darwin regional traditional customary associations  
151 with Country, including within the Howard River area and Girraween Lagoon catchment  
152 (Burns 1999; Wells, 2001). Wells (2001) provides an account of Darwin history from a  
153 Larrakia perspective.

154

## 155 **Methods**

156           Girraween Lagoon was cored using a floating platform with hydraulic coring-rig. A  
157 19.4 m core in 1 m sections was collected to the point of bedrock. The focus of this paper is  
158 the 478–598 cm section encompassing the LGM as well as the interval immediately before  
159 and after the LGM. Details and imagery of field, laboratory and microscope methods are  
160 reported in Rowe et al. (2019a, 2019b).

161

### 162 *Pollen and charcoal analysis*

163           Two cubic centimeter sediment samples were processed for pollen and  
164 microcharcoal analysis. Sample preparation followed the techniques as detailed in Rowe et al.



165 (2019a, b; see also references used therein). Chemical preparations (including Na<sub>4</sub>P<sub>2</sub>O<sub>7</sub>,  
166 KOH, HCl, acetolysis and C<sub>2</sub>H<sub>5</sub>OH washes) were selected to initially disperse the organic-  
167 mineral matrix then progressively remove humic acids, calcium carbonates, bulk (in)organics,  
168 and silicates, as well as to render pollen ornamentations visible. Sieving took place at 7 µm  
169 and 125 µm. A *Lycopodium* spike (Lunds University batch 3862) was added during  
170 laboratory preparations, to determine concentrations of pollen and microcharcoal particles.  
171 Final residues were mounted in glycerol. Pollen counts are a minimum of 150 grains  
172 (including spores) per sample (single sample exception identified and described below).  
173 Pollen identification was based upon regionally representative floral reference libraries in  
174 development by the lead author (CR), and on online resources including the Australasian  
175 Pollen and Spore Atlas (<http://apsa.anu.edu.au/>). For additional information on Myrtaceae  
176 pollen identification, refer to Stevenson et al. (2015).

177           Insight into plant ecologies was gained through sources such as FloraNT  
178 ([eflora.nt.gov.au](http://eflora.nt.gov.au)). All data were plotted using TGView (Grimm, 2004). A dendrogram  
179 produced by CONISS (Grimm, 1987; 2004) was used to help in selection of diagram zone  
180 boundary location. Pollen was divided into eight groups to capture plant form and/or  
181 vegetation type. These groups were then classified further and allocated into plant-function  
182 and/or environmental response categories: dryland and wetland associated Myrtaceae, other  
183 woody taxa (sclerophyll or monsoonal forest affiliated), Poaceae, herbaceous taxa,  
184 pteridophytes and wetland associates (plant terms ‘wetland’ and ‘aquatic’ are used in reference  
185 to areas of seasonal versus permanent inundation, respectfully). These groups were then  
186 condensed further, and pollen allocated into plant-function and/or environmental response  
187 categories. Such categories helped evaluate fire tolerances as well as assess wet–dry  
188 continuums. Rowe et al. (2019a) provide an extended discussion on the allocation and use of  
189 plant functional types for the Girraween pollen record. All pollen types are identified to the

190 most refined taxonomic level possible. In certain cases (e.g., Fabaceae, Myrtaceae) grain  
191 morphological descriptors are included in the categorisations to help highlight differing grain  
192 types. Accounting for pollen types in this way ensures diversity within the record is not lost.  
193 Microcharcoal particles (black, opaque, angular, >10  $\mu\text{m}$  in length) were counted  
194 simultaneously with pollen and as an indicator of landscape fire. Charcoal, as a proxy for  
195 local to regional fire occurrence, is guided by the advice of Whitlock and Larsen (2001) and  
196 as used in Rowe et al. (2019a).

197

### 198 *Hydrogen pyrolysis of stable polycyclic aromatic carbon*

199         Fifteen samples from a subset of depth intervals were analysed for the abundance  
200 and carbon isotope composition of total organic carbon (TOC) and pyrogenic carbon (PyC),  
201 by hydrogen pyrolysis (HyPy). HyPy quantifies PyC present as stable polycyclic aromatic  
202 carbon (SPAC) which has been shown to comprise compounds of more than seven condensed  
203 polycyclic aromatic rings (Meredith et al., 2012; Wurster et al., 2012, 2013). The technique  
204 has been described in detail in a number of publications (e.g., Ascough et al., 2009; Meredith  
205 et al., 2012). Briefly, 25–100 mg aliquots of each sample were loaded with a molybdenum  
206 (Mo) catalyst using an aqueous/methanol (1:1) solution of ammonium dioxodithiomolybdate  
207  $[(\text{NH}_4)_2\text{MoO}_2\text{S}_2]$ . Catalyst weight was ~10% sample weight for all samples to give a nominal  
208 loading of 1% Mo. After sample loading, the reactor was pressurized with hydrogen to 15  
209 GPa with a sweep gas flow of 5 L  $\text{min}^{-1}$ , then heated using a pre-programmed temperature  
210 profile, where samples are initially heated at a rate of 300°C  $\text{min}^{-1}$  to 250°C, then heated at a  
211 rate of 8°C  $\text{min}^{-1}$  until the final hold temperature of 550°C for 5 min.

212         Carbon abundance and isotope composition of samples were determined using a  
213 Costech Elemental Analyzer fitted with a zero-blank autosampler coupled via a ConFlow

214 4010 to a ThermoFinnigan DeltaV<sup>PLUS</sup> using Continuous-Flow Isotope Ratio Mass  
215 Spectrometry (CF-IRMS) at the Advanced Analytical Unit at James Cook University, Cairns.  
216 Stable isotope results are reported as per mil (‰) deviations from the Vienna Pee Dee  
217 Belemnite (VPDB) reference standard scale for  $\delta^{13}\text{C}$  values. Precisions ( $\sigma$ ) on internal  
218 standards were better than  $\pm 0.1\%$ .

219

### 220 *Radiocarbon dating and age model development*

221 Four samples of bulk sediment from above, within, and below the LGM section of  
222 the core were pre-treated by hydrogen pyrolysis to remove labile carbon from pyrogenic  
223 carbon (charcoal) component for radiocarbon dating. The protocol used was identical to that  
224 described in Rowe et al. (2019a, b). Pre-treated samples were then combusted to  $\text{CO}_2$  and  
225 reduced to a graphite target for measurement at ANSTO, as reported in Bird et al. (2014).  
226 Age reporting follows Stuiver and Polach (1977), converted into calibrated ages using CALIB  
227 REV7.1.0 (Stuiver and Reimer, 1993, Hogg et al., 2013; calibration curve SHCal13). A  
228 Bayesian age-depth model was constructed for the LGM interval of core using Bacon 2.2  
229 (Blaauw and Christen, 2011).

230

## 231 **RESULTS**

### 232 **Chronology and sedimentology**

233 The depth interval of interest here incorporates two radiocarbon results. However,  
234 the overall modelled calibrated chronology is based on four radiocarbon measurements, using  
235 samples above and below our interval of interest, from the same core. All sample depths,  
236 percent modern carbon (pMC), conventional (yr BP) and calibrated (cal yr BP) radiocarbon  
237 ages are listed in Table 1, with the two radiocarbon results pertaining to this study highlighted

238 in grey. The lowermost sample in the interval under consideration in this paper (595 cm) was  
239 modelled to ~26,500 cal yr BP, while the uppermost sample at 478 cm was modelled to  
240 18,500 cal yr BP (Fig. 2). The interval thus encompasses a period of 8000 years, with the  
241 LGM ( $21,000 \pm 2000$  calendar years) represented by samples between 485 cm and 518 cm.  
242 The age model in this study differs from that presented in Rowe et al. (2019a) due to  
243 subsequent sub-sampling and availability of OZV443 and OZU820 (Table 1).

244 Sediments are consistent throughout this section of the core, described as dark olive-  
245 grey (5Y, 3/2 per Munsell color charts) consolidated and fine clay with decomposed (sapric)  
246 organic material. While there is no change in the nature of the sediments in the LGM,  
247 sedimentation rate decreases substantially into the LGM (Fig. 2).

248

#### 249 **Palynological analysis**

250 Sixty pollen taxa were identified in the end-phase last glacial pollen and  
251 microcharcoal from Girraween (Fig. 3a, b, c). Unidentified pollen accounted for an average  
252 9% of sample pollen counts. One sample demonstrated low pollen preservation (490 cm,  
253 19.96 cal ka BP) and was excluded from the analysis. Three pollen zones are illustrated; a  
254 lower zone labelled GIR-1 (598–524 cm below sediment surface [bss]; ca. 26.53–23.75 cal ka  
255 BP), a middle zone labelled GIR-2 (524–493 cm bss; ca. 23.75–20.3 cal ka BP), and an upper  
256 zone labelled GIR-3 (493–478 cm bss; ca. 20.3–18.5 cal ka BP).

257 Zonation was assisted by the numerical classifications. For example, GIR-3 samples  
258 have been separated due to very similar values for the three main taxa (*Myrtaceae*–  
259 *Eucalyptus*, *Poaceae* and *Cyperaceae*). Zone GIR-1 has been further divided into sub-zones,  
260 determined largely by variations in herbaceous pollen (GIR-1a, 598–586 cm bss, ca. 26.53–  
261 26.2 cal ka BP; GIR-1b, 586–538 cm bss, ca. 26.2–24.5 cal ka BP; GIR-1c, 538–524 cm bss,

262 ca. 24.5–23.75 cal ka BP). Secondary zonation influences include differences in non-  
263 Myrtaceae woody plants. The lower two major zones also show an upward overall decline in  
264 charcoal accumulation, crossing over into zone GIR-3 with a sharp increase before decreasing  
265 toward the top of the core. A spike in charcoal at 496 cm is the one exception to trends in  
266 glacial burning.

267

268 *Zone GIR-1 598–524 cm bss, ca. 26.53–23.75 cal ka BP*

269         Zone GIR-1 is dominated by Poaceae (65–82% of the pollen sum), and further  
270 characterised by variable total values (and composition) in the minor dryland plant groups, as  
271 also reflected in the pollen richness index. Zone GIR-1 contains a high number of  
272 Melaleuceae, woody sclerophyll-monsoonal forest taxa (non-eucalypts) and herbaceous  
273 pollen types, notably within subzone GIR-1b (26.2–24.5 cal ka BP), after which a number of  
274 plants are lost from the record. The representation of minor plant groups and associated  
275 diversity decline into subzone GIR-1c (24.5–23.75 cal ka BP), and with relative similarity  
276 continuing into zone GIR-2. Upper subzone GIR-1c into zone GIR-2 represents a transitional  
277 phase into the LGM.

278         Larger sized Myrtaceae pollen (grain morphology observed as the eucalypts within  
279 the tribe Eucalypteae, see Thornhill et al., 2012; and the author CR's previous Myrtaceae  
280 pollen analysis in Stevenson et al., 2015) represent the main tree signal ( $\leq 12\%$  of the pollen  
281 sum, decreasing to 1.5% at 24.6 cal ka BP) and mixed with sparse sub-canopy tree taxa,  
282 including *Brachychiton* and *Casuarina*, and likely shrub types, Malvaceae, Fabaceae and  
283 Arecaceae (all  $< 2\%$ ). Monsoonal-forest affiliated Moraceae, *Celtis*, *Timonius*, *Myristica* and  
284 *Trema* co-occur in low abundances (also all  $< 2\%$ ). Amaranthaceae/Chenopodiaceae  
285 (combining *Gomphrena* and *Atriplex-Ptilotus* pollen types) are the major herbaceous taxon

286 (up to 14%), but gradually decline toward zone GIR-2. Other herbs (12 total sub-shrubs and  
287 forbs) are sporadic when present.

288           Zone GIR-1 charcoal records fluctuate, with higher accumulations through subzone  
289 GIR-1b (26.2–24.5 cal ka BP). Increases in particles occur at 26.1, 25.8 and 24.6 cal ka BP;  
290 greater charcoal coincides with higher and ongoing herbaceous occurrence and expansions in  
291 non-eucalypt woody taxa. High zone GIR-1 charcoal is recorded alongside woody (e.g.,  
292 *Dodonaea*) and herbaceous (e.g., *Euphorbia*) taxa favoured by disturbance, particularly fire  
293 (Moore, 2005; Hyland et al., 2010), as well as known open and drier habitat herbaceous ‘fire  
294 weeds’ (e.g., *Solanum*; Moore, 2005).

295           The Cyperaceae (sedge) family and similarly grouped wetland plants such as  
296 *Caldesia* are consistently low (<5% of the pollen sum). No aquatic taxa are recorded. Ferns  
297 are occasional, and absent in subzone GIR-1c.

298

299 *Zone GIR-2 524–493 cm bss, ca. 23.75–20.3 cal ka BP*

300           The bulk of zone GIR-2 encompasses the LGM. Dominant Poaceae pollen  
301 percentages continue through this zone (66–76%), and combine with lower proportion, more  
302 fluctuating, and less diverse minor plant groups. Woody taxa in all ecological categories show  
303 more irregular appearance and abundance than herbaceous plants. When recorded, the  
304 eucalypts (0.5–18%) remain the primary sclerophyll tree canopy component, with sub-canopy  
305 composition including *Terminalia*, *Acacia*, *Pandanus*, *Hakea* and Fabaceae shrubs such as  
306 *Daviesia*. Other members of the Fabaceae family, as well as trees such as *Casuarina*,  
307 disappear beginning 20.7 cal ka BP. *Timonius*, *Myristica* and *Trema* remain, and taxa  
308 *Melastoma* and Euphorbiaceae-*Macaranga* appear in the record to characterise a monsoonal-

309 forest signal (all <2–4%). No lianas are represented within the forest group. Non-eucalypt  
310 pollen outnumbers eucalypt pollen at 23.5 cal ka BP and 22.4 cal ka BP.

311 As ground cover, Amaranthaceae/Chenopodiaceae types maintain presence (ca. 4%)  
312 until 21.6 cal ka BP. Herbs such as *Solanum*, *Euphorbia*, and potential Fabaceae types occur  
313 in low abundances, also until 21.6 cal ka BP, after which herbaceous taxa are not recorded  
314 until the top of the core. Fern spore values remain low. Wetland elements are similar or  
315 slightly higher than in zone GIR-1 and primarily composed of Cyperaceae. Cyperaceae  
316 combine with Melaleuceae foremost in the upper part of this zone. A single record of aquatic  
317 pollen occurs at 22.4 cal ka BP (*Nymphoides*, <1%).

318 The scale of zone GIR-2's charcoal accumulation is skewed toward a single peak  
319 sample, dated to 20.7 cal ka BP at the top of the zone. Charcoal results are otherwise low and  
320 consistent comparative to zone GIR-1.

321

322 *Zone GIR-3 493–478 cm bss, ca. 20.3–18.5 cal ka BP*

323 The sample at 490 cm depth (age 20 cal ka BP) showed very poor pollen  
324 preservation. Vegetation shifts and fire patterns are therefore interpreted with caution.  
325 Diversity values are lowest for the record and the majority of plant groups are not recorded.  
326 Pollen is dominated by near-even percentages of grass and eucalypts; Cyperaceae  
327 (comprising *Cyperus* only) otherwise rise.

328 The top-most sample (478 cm, 18.5 cal ka BP) is contemporaneous with early-stage  
329 deglaciation. Eucalypt values increase from zone GIR-2 (to 22%), and combine with greatest  
330 presence (9.5%) sclerophyll sub-canopy woody taxa. Sub-canopy composition is a  
331 continuation of that established in zone GIR-2 (*Terminalia*, *Acacia*, *Pandanus*, *Hakea* and  
332 Fabaceae shrubs, each at higher individual values), with the reappearance of *Petalostigma* and

333 Arecaceae from before the LGM. Forest associated taxa are absent. Herbaceous, sedge and  
334 fern diversity is low. A decline in Poaceae suggests vegetation structure is less open.

335 Charcoal accumulations progressively decline from the peak observed at 20.7 cal ka  
336 BP achieving values similar to the remainder of the record.

337

### 338 **Pyrogenic carbon**

339 TOC abundances are uniformly low and relatively constant through the examined  
340 interval (from 0.37 to 0.64%, Fig. 3a). PyC mass accumulation rate decreases from 33–58  
341  $\mu\text{g}/\text{cm}^2/\text{yr}$  before and into the interval identified as the LGM and is relatively stable through  
342 and beyond the interval identified as the LGM, with fluxes of 9–22  $\mu\text{g}/\text{cm}^2/\text{yr}$ . The  $\delta^{13}\text{C}$   
343 values of TOC exhibit a relatively narrow range from -14.7‰ to -16.1‰, indicating a  
344 substantial  $\text{C}_4$  component, with no overall trend through the interval. The  $\delta^{13}\text{C}$  values of PyC  
345 are generally lower than TOC, with a substantially greater range from -14.6‰ to -23.3‰.  
346 Overall, there is an irregular trend from lower  $\delta^{13}\text{C}$  values (generally  $<-20\text{‰}$ ) prior to and at  
347 the start of the LGM, with higher values ( $>-20\text{‰}$ ) toward the end of the LGM and continuing  
348 into the post-glacial period.

349

## 350 **DISCUSSION**

### 351 **Vegetation dynamics**

352 Pollen indicates that vegetation characterised by grasses with sparse trees and shrubs  
353 occupied Girraween's catchment through the period 26.5–18.5 cal ka BP. While grass  
354 communities were the most extensive and continuous pollen-plant group across the area, at no  
355 time was the vegetation grass only. This conclusion is supported by high  $\delta^{13}\text{C}$  values in TOC



356 in the sediments throughout the interval under investigation which remain always higher than  
357 -16.1‰. This indicates a dominant but not exclusive C<sub>4</sub> (grass) contribution to organic carbon  
358 in the sediments. A significant C<sub>4</sub> component also contributed to the PyC preserved in the  
359 lake sediment, but δ<sup>13</sup>C values are lower than for TOC, again indicating that the region was  
360 exclusively C<sub>4</sub> (discussed below). Grasses did not extensively co-exist with other ground  
361 layer taxa. Although monsoonal-forest taxa (semi-deciduous trees and shrubs, and other  
362 tropical elements including Areaceae and lianas) occurred, *Eucalyptus* species (notably *E.*  
363 *tetrodonta*) dominated the tree layer throughout the record, and the woody vegetation was  
364 therefore predominantly sclerophyllous. Wetland-associated plants were not widespread  
365 landscape components and their presence was determined by localised sinkhole site  
366 characteristics.

367         Preceding the LGM, from 26.6 cal ka BP, grasses were abundant and accompanied  
368 by few eucalypts. Vegetation structure showed little sub-canopy layering, with non-eucalypt  
369 tree-shrubs sparingly represented and largely consisting of *Petalostigma*. Eucalypts are the  
370 only recorded woody taxon at 26.2 cal ka BP. A small range of herbs consisted of  
371 Amaranthaceae-Chenopodiaceae types and Asteraceae. After 26.2 cal ka BP the variety of  
372 non-eucalypt trees and shrubs (e.g., *Brachychiton*, *Casuarina*, *Dodonaea*; and monsoonal-  
373 forest associated *Celtis*, *Trema* and *Myristica*) increased, but given ongoing high  
374 representation of grass pollen, vegetation structure remained very open. Along with Poaceae,  
375 understories incorporated a more mixed suite of herbs; foremost after 26.2 cal ka BP  
376 Amaranthaceae-Chenopodiaceae (*Ptilotus-Atriplex*, *Gomphrena*) increased, with other herbs  
377 (e.g., *Spermacoce*, Polygonaceae, *Evolvulus*) common in various combinations. The  
378 herbaceous group may have formed its own small plant associations, as for example within  
379 modern inland-arid Australia many forbs are observed to accompany Chenopodiaceae  
380 (Moore, 2005).

381 Transition toward the LGM is evident from 25.3 cal ka BP with the loss of many  
382 sub-canopy trees and shrubs, thinning again at 24.9 cal ka BP by the disappearance of  
383 numerous minor herbs, and at 24.5 cal ka BP when Amaranthaceae-Chenopodiaceae began to  
384 decline. At this same latter time eucalypt presence decreased. Within the formally defined  
385 LGM period ( $21 \pm 2$  ka BP) the exclusion of herbs is dramatically evident and grasses  
386 achieved maximum abundance (22.4 cal ka BP; 77%). Woody components, including  
387 eucalypts, fluctuated to an extent not previously seen, and a shift occurred in the composition  
388 of sub-canopy non-eucalypts, combining sparse (but more dry adapted, Moore, 2005) *Acacia*,  
389 *Terminalia*, *Hakea* and Fabaceae, with declining monsoonal-forest types. This dryland  
390 composition, and also fluctuations in these taxa—of eucalypts in particular—was maintained  
391 through the deglaciation until the Holocene, at which time mixed woody cover increased to  
392 the point of establishing as open forest (Rowe et al., 2019a).

393 Fire occurred consistently through the entire period, but charcoal particle flux was  
394 significantly less than observed during the Holocene (Rowe et al., 2019a), implying  
395 comparatively reduced fire activity consistent with significantly lower biomass available to  
396 burn. Small increases in fire are evident between 26.2–24.5 cal ka BP, and more dramatically  
397 at 20.7 cal ka BP. The PyC fluxes and PyC  $\delta^{13}\text{C}$  values shed additional light on fire regime  
398 through the interval. Unlike the charcoal particle fluxes, PyC flux decreases through GIR  
399 zone 1 and remains low in the LGM (GIR zone 2) and immediate post-glacial (GIR zone 3).

400 Whereas particle counting records all charred particles, not all charred particles will  
401 be identified as PyC. Wurster et al. (2013) found almost no PyC was produced by hydrogen  
402 pyrolysis at temperatures below  $\sim 350^\circ\text{C}$ , with  $\sim 50\%$  of charred carbon being identified as  
403 PyC by  $500^\circ\text{C}$ , and the majority of carbon present as PyC by  $\sim 700^\circ\text{C}$ , which was confirmed  
404 by McBeath et al. (2015). This implies that the relative difference in trends between particle

405 and PyC fluxes can be interpreted as a relative difference in fire intensity. Thus, fire intensity  
406 in GIR Zone 1 (pre-LGM) was initially the highest across the interval examined herein, but  
407 declined and stabilized into the LGM. The comparatively high charcoal particle fluxes in  
408 upper GIR Zone 2 and lower GIR Zone 3 are not accompanied by increased PyC fluxes,  
409 implying relatively low fire intensity. These trends may have been driven simply by declining  
410 biomass and fuel connectivity into the LGM. The PyC  $\delta^{13}\text{C}$  values are lower than TOC  $\delta^{13}\text{C}$   
411 values, indicating that a substantial fraction of  $\text{C}_4$  biomass was completely combusted (or  
412 exported as fine aerosol particles) with the char remaining after fires biased toward  
413 woody/herbaceous ( $\text{C}_3$ ) particles as has been observed in modern savanna environments (Saiz  
414 et al., 2015). PyC  $\delta^{13}\text{C}$  values do increase irregularly through the entire interval under  
415 investigation, implying a slight increase in the proportion of  $\text{C}_4$  biomass contributing to the  
416 PyC preserved in the record. This is consistent with the slight increase in the proportion of  
417 Poaceae pollen (largely at the expense of herbaceous pollen) into the LGM (Fig.s 3a, b, c).

418

#### 419 **Taxon observations**

420 When compared to modern site observations (Schult, 2004), reference pollen data for  
421 the NT (Bird et al., 2019), and Holocene ecology (Rowe et al., 2019a, b), Girraween's woody  
422 vegetation was less diverse and reduced markedly, but not removed entirely, under glacial  
423 conditions. With broad-based estimates of LGM tropical temperatures 3–6°C cooler (Prentice  
424 et al., 2017) and weakened hydrological cycles unfavourable for precipitation (Liu, 2018; p.  
425 363) a biogeographic boundary shift occurred across the Darwin region, whereby open  
426 xerophytic grassy-savanna similar to that from the NT's continental interior (see Moore,  
427 2005) encroached on a region that is currently mesic-woody-savanna. Key responses at  
428 Girraween were high grass representation compared to woody plants, compositional shifts to

429 woody and non-woody dry-adapted taxa, and less plant diversity with restricted wetland  
430 affiliates.

431 Woody biomass and diversity in modern Australian savannas are influenced by  
432 water stress (plant available moisture, driven by annual rainfall total and delivery pattern,  
433 including dry season length and regularity of storms, Cook et al., 2002; Cook and Heerdegen,  
434 2001). Mapped against declining moisture with distances inland (North Australian Tropical  
435 Transect, see also Beringer et al., 2011), Murphy et al. (2015) observe tree loss as well as  
436 reduced tree diversity. Hutley et al. (2011) further describe declines in individual tree  
437 performance, as measured by stem density, overstorey leaf-area and canopy height. Reduction  
438 in these woody structural attributes is interpreted to have occurred alongside site losses of  
439 woody taxa through a drier and cooler last glacial at Girraween.

440 LGM atmospheric CO<sub>2</sub> concentrations were 185 parts-per-million (ppm), compared  
441 with 280 ppm pre-industrial values (Schmitt et al., 2012; Calvo and Prentice, 2015). Claussen  
442 et al. (2013) emphasise the synergy between last glacial climate and ecophysiological CO<sub>2</sub>  
443 impact. In this respect, where glacial climate change influenced NT ecosystem boundaries  
444 (plant dispersion), lower CO<sub>2</sub> concentrations invoked C<sub>3</sub>-C<sub>4</sub> plant competition, further  
445 modifying growth patterns of different plant functional types at Girraween. Prentice and  
446 Harrison (2009) highlight low CO<sub>2</sub> individual plant physiological consequences scale up to  
447 major ecosystem effects.

448 At low CO<sub>2</sub> levels, woody C<sub>3</sub> photosynthetic pathways are reduced. In consequence,  
449 transpiration and water-use efficiency decrease (Claussen et al., 2013). C<sub>3</sub> plants grown  
450 experimentally at low Pleistocene CO<sub>2</sub> levels show strong evidence of stress, including  
451 biomass production diminished up to 90% relative to that of plants grown at current  
452 atmospheric CO<sub>2</sub>. Low CO<sub>2</sub> has also been shown to reduce or prevent reproduction in C<sub>3</sub>

453 species, whereas growth and reproduction of C<sub>4</sub> species (e.g. tropical grasses) are generally  
454 unaffected (Ward et al., 2001 and references therein). As a result, there are two explanations  
455 for the dominance of C<sub>4</sub> grasses during the last glacial: low CO<sub>2</sub> and drier climate. Grasses  
456 would have benefited even further without extensive shading and leaf-litter to negatively  
457 affect life-cycle stages such as germination (Scott et al., 2009). Impacts on tree stands include  
458 reduced net primary productivity as a result of lower CO<sub>2</sub>, enhanced tree-tree competition,  
459 and favoured deciduous over evergreen leaf-trait behaviour (Harrison and Prentice, 2003;  
460 House et al., 2003).

461           Between 26.5–18.5 cal ka BP, eucalypts were the main woody taxon through their  
462 competitive advantage for water (eucalypts are drought tolerant, Boland et al., 2002, and see  
463 Prior, 1997, for *E. tetradonta*). Eucalypts are also known for high capacities to grow through  
464 savanna fire cycles (Murphy et al., 2015). An evergreen monsoonal-forest community at  
465 Girraween was unlikely at the last glacial, including at the LGM. Environmental tolerances  
466 shown by individual forest-aligned taxa are wider than the forested-type vegetation  
467 communities formed by combinations of such taxa (Speck et al., 2010). Abilities to regulate  
468 water usage as drought-evading plants (including semi-deciduous, larger seed-size, seed  
469 dormancy and/or deep-rooting behaviours; Grubb and Metcalf, 1996; Brock, 2001; Moore,  
470 2005; Jeremy Russell-Smith and Setterfield, 2006), helps explains the presence of *Timonius*,  
471 *Celtis*, *Trema*, Moraceae (e.g., *Ficus*), Areaceae (e.g., *Livisonta*), and *Macaranga*, as well as  
472 *Terminalia* and *Brachychiton*. It positions them as intermediate taxa within the eucalypts at  
473 Girraween (cf. Speck et al., 2010). While water scarcity by itself appears unlikely to have  
474 been critical for forest taxa tolerant of drought, it (in combination with low CO<sub>2</sub>) likely  
475 rendered them inferior eucalypt competitors (Murphy et al., 2015; House et al., 2003).  
476 Vulnerability to fire may also have been enhanced (see below; Brock, 2001).

477           Woody taxa are rarely continuously maintained for more than one sample (Fig. 3b).  
478 This data pattern continues into the early stages of the Holocene (Rowe et al., 2019a, and  
479 Figs. 2b and c), and variations in pollen counts are acknowledged as much as actual variation  
480 in plant abundance. The speculation here is that plants are capable of episodic growth  
481 responses following potential periodic monsoon-moisture availability, but do not demonstrate  
482 long-term recovery and expansion suggestive of an overall long-term unfavourable climate.  
483 Rapid responses, as well as short-lived taxa such as *Macaranga* and Fabaceae types are  
484 indicative of an overall increase in ecosystem turnover rates under the influence of glacial to  
485 post-glacial to early Holocene conditions (cf. Haberle, 2005). The extent of glacial climatic  
486 and low CO<sub>2</sub> driven woody suppression is also evident, where low fire frequency is otherwise  
487 associated with tree-shrub recruitment (canopy and/or sub-canopy development, Scholes and  
488 Archer, 1997; Scott et al., 2009). Taking further cues from the modern NT interior (see  
489 above; Moore 2005; Hutley et al., 2011), at Girraween woody plants may have occurred as  
490 scattered individuals above the grasses. Mixed composition discrete woody vegetation  
491 structures potentially existed as fragments of woodland which persisted from earlier periods  
492 of more favourable climate within habitat pockets. Grouping of woody plants may also have  
493 developed in relation to fire events.

494           The combined effect of relatively lower glacial precipitation, cool temperatures, low  
495 CO<sub>2</sub>, and lower biomass of sclerophyll woodland would have been sufficient to dramatically  
496 reduce charcoal deposition. Comparison with Rowe et al. (2019a) and Bird et al. (2019)  
497 suggests Girraween had a lower capacity to carry fire, and was subject to a relatively uniform  
498 fire regime during the LGM. Savanna studies refer to fire as a top-down factor influencing  
499 grass-woody layer compositions as opposed to bottom-up environmental factors such as  
500 plant-available moisture and edaphic properties (Scholes and Archer, 1997; Scott et al.,  
501 2009). The results of this study suggest top-down fire processes played less of a role in the

502 LGM in determining vegetation than in the Holocene and modern day. Grasses in the LGM  
503 were little affected by burning; eucalypts were also unresponsive. Fire appears to have  
504 exerted only selective influence on minor woody plant groups such as the non-eucalypts and  
505 herbs. As one theory, low-level fire potentially assisted to release nutrients into an overall  
506 nutrient deficient savanna ecosystem (Richards et al., 2011; Cook, 1994), to benefit restricted  
507 and/or lesser-drought-tolerant taxa. The germination of herbs can also be favoured by heat  
508 and smoke after burning, and fire can promote flowering (Fensham et al., 2002; Nano and  
509 Clarke, 2011; and under less intense fire as defined by Richards et al., 2011, p. 504).

510 . We conclude that glacial climate change and CO<sub>2</sub> effects were primary factors  
511 dictating Girraween's vegetation structure and composition, and were also the primary factors  
512 influencing fire in the region. Site characteristics were a secondary determinant. The sinkhole  
513 depression would vary in microclimate, soil types, water drainage, and potentially be less  
514 exposed to fire than the wider landscape, thereby providing a major source of pocket habitats  
515 for plants. This would have been the primary influence on the presence and distribution of  
516 wetland plant assemblages during the end-stage glacial and LGM, and the location from  
517 which wetland plants expand during deglaciation. Taxa such as *Melaleuca*, *Cyperaceae*  
518 (*Cyperus*, *Eleocharis/Schoenus*, *Fimbristylis*), *Caldesia* and the Pteridophyta were more  
519 likely to be located within the depression adjacent to the sinkhole than to occupy the open  
520 grassy catchment. The surrounding catchment was a drier, more exposed, and more uniform  
521 habitat. This limited wetland-related flora, which was unable to effectively compete with dry-  
522 resisting or dry-evading taxa, woody and non-woody alike. Any plant within the sinkhole  
523 would in turn provide a surface-stabilising effect, generally capable of protecting depression  
524 slopes from erosion. The sinkhole waterbody did not support an aquatic plant community.  
525 Glacial stage drawdowns likely affected aquatic plants directly through exposure to aerial  
526 conditions and indirectly through substrate modification. Droughts and/or limited water

527 exchange can produce anoxic (reducing) conditions that are toxic to many water plants  
528 (Santamaria, 2002; Bornette and Puijalon, 2011). As per slow decomposition of dryland soil  
529 organic matter, cooler water temperatures also slow down the mineralisation of organic  
530 matter, impeding nutrient release into the water column for taxa such as *Nymphaea* (Bornette  
531 and Puijalon, 2011).

532

### 533 **Climate inferences**

534         The palynological results presented here along with an understanding of the coastline  
535 position at the LGM enable a semi-quantitative estimate of annual rainfall at Girraween  
536 Lagoon during the LGM. The coastline was approximately 300 km north and northwest of the  
537 site during the LGM (Ishiwa et al., 2019). Assuming no diminution of monsoon intensity and  
538 applying the modern continental rainfall gradient would imply that rainfall was diminished  
539 from 1700 mm to approximately 1000 mm (Cook and Heerdegen, 2001). Also by analogy  
540 with modern climate in the region, seasonality would be increased with duration of the rainy  
541 season decreased from 200 days to 150 days (Cook and Heerdegen, 2001).

542         *E. tetradonta* pollen is not common but remains represented in LGM samples (Fig.  
543 3b). This species is relatively common in regions with ~700 mm annual rainfall (Boland et  
544 al., 2006) with exceptional occurrences down to 500 mm. This does not take into account the  
545 effect of either decreased CO<sub>2</sub> or temperature during the LGM on species distribution,  
546 however these changes act in opposite directions on vegetation. Decreased CO<sub>2</sub> is likely to  
547 have decreased the competitiveness of woody C<sub>3</sub> biomass compared to grass-dominated C<sub>4</sub>  
548 biomass (Prentice et al., 2017). Decreased LGM temperature, the magnitude of which is  
549 poorly constrained in the study region (e.g., Cleator et al., 2019) would decrease evaporation  
550 and therefore increase effective plant available moisture for a given mean annual rainfall (Liu



551 et al., 2018). By combining coastline position and *E. tetradonta* rainfall requirements we thus  
552 conclude that mean annual rainfall at Girraween Lagoon was most likely in the range 700-  
553 1000 mm (Fig. 4).

554 Our results are generally consistent with recent modelling results for the LGM  
555 globally (Jiang et al., 2015) and for the northern Australian region (Yan et al., 2018). These  
556 studies indicate that there was still an effective monsoon rainfall regime across the northern  
557 Australian region, in accordance with earlier studies (e.g. Marshall and Lynch, 2008). Yan et  
558 al. (2018) conclude that changes in land-sea distribution and east-west gradients in sea surface  
559 temperature resulted in a modest lowering of total rainfall but an increase in rainfall  
560 seasonality across northern Australia, again in accord with previous studies (Marshall and  
561 Lynch, 2008). These results suggest that a value towards the lower rainfall boundary  
562 suggested above is more likely than the upper rainfall boundary and that the monsoon season  
563 duration of 150 days inferred above is more likely an upper boundary.

564 Jiang et al. (2015) specifically note a lack of correspondence between their  
565 modelling results and conclusions based on (very sparse) northern Australian climate proxy  
566 records for the LGM. This appears to largely be an artefact of terminology. The LGM  
567 coastline was between 200 and 500 km seaward of the modern coastline along the entire  
568 length of western northern Australia (Fig. 1), and this means that the change in coastline  
569 position will have dramatically decreased precipitation at any terrestrial site simply due to the  
570 strong rainfall gradient into the interior. A corollary of this is that monsoon rainfall may not  
571 have penetrated far into south-draining catchments, and hence low lake levels are recorded in  
572 the arid northern Australian interior at the LGM (e.g., Fitzsimmons et al., 2012). So while the  
573 modern Australian terrestrial region was more arid at the LGM, this does not imply monsoon  
574 failure, but more likely a shift of the majority of monsoon rainfall onto the now-flooded  
575 continental shelf. Palynological investigation of deep sea cores between Australia and New

576 Guinea, which therefore were exposed to pollen rain from the exposed continental shelf of  
577 Australia, do show an expansion of grassland at the LGM (e.g., van der Kaars, 1991). This  
578 suggests that some combination of rainfall amount, seasonality, reduced CO<sub>2</sub> and reduced  
579 temperature did lead to a general reduction in tree cover over that expected simply from the  
580 operation of a continental rainfall gradient similar to that currently observed.

581

## 582 **CONCLUSIONS**

583           Girraween Lagoon remained a perennial water body throughout the LGM and as a  
584 result retains a proxy record of the LGM environment. The palynological results for the LGM  
585 interval indicate a dramatic reduction in tree cover and expansion of grassland relative to  
586 current tall woodland vegetation at the site. Dryland vegetation during the LGM interval is  
587 best described as an open xerophytic grassy-savanna. In terms of the megabiome  
588 classification of Dallmeyer et al. (2019), the site is likely on the boundary between  
589 grassland/dry shrubland and savanna/dry woodland. In other DGVM classification schemes  
590 the Girraween site is best characterized as close to the boundary of plant functional types  
591 variously described as grassland, xerophytic shrubland, grassland/shrubland, and tropical  
592 savanna (e.g., Calvo and Prentice, 2015).

593           No inference can be drawn with respect to LGM temperature at the site, but rainfall  
594 may be constrained to 700–1000 mm, more likely toward the lower than the upper bound, and  
595 wet season length was likely <150 days. The monsoon remained active but most monsoon  
596 rainfall fell on the now-flooded continental shelf as a result of a steep rainfall gradient into the  
597 continental interior, similar to that which pertains today.

598           Girraween Lagoon and other permanent water bodies in the Darwin region would  
599 have enabled continued human occupation of the area through the LGM, although there is  
600 currently no dated evidence of human activity in the region at that time.

601

## 602 **ACKNOWLEDGMENTS**

603 This research was funded by the Australian Research Council Centre of Excellence for  
604 Australian Biodiversity and Heritage (CE170100015) and an Australian Research Council  
605 Laureate Fellowship to M.I.B. (FL140100044). L.H. is recipient of Discovery Project  
606 DP130100334. V.L. acknowledges the financial support from the Australian Government for  
607 the Centre for Accelerator Science at ANSTO, where the measurements were done, through  
608 the National Collaborative Research Infrastructure Strategy (NCRIS), and expresses gratitude  
609 to the radiocarbon laboratory staff who processed our samples. Rainy Comley's assistance  
610 within the JCU laboratories was greatly appreciated. Warm thanks to the Larrakia Nation,  
611 Larrakia Ranger group, and the wider Larrakia community for their support and local insights  
612 into the Girraween environment. Access assistance from Graham Churcher is also gratefully  
613 acknowledged. Thanks also to Ron Innes for engineering work on the raft and coring  
614 equipment. The authors also appreciate the feedback provided by two reviews on earlier  
615 drafts.

616

## 617 **REFERENCES**

618 Alder, J.R., Hostetler, S.W., 2015. Global climate simulations at 3000-year intervals for the  
619 last 21000 years with the GENMOM coupled atmosphere-ocean model. *Climate of the*  
620 *Past* 11, 449-471.

621 Ascough, P. L., Bird, M. I., Brock, F., Higham, T. F. G., Meredith, W., Snape, C. E., Vane, C.  
622 H., 2009. Hydropyrolysis as a new tool for radiocarbon pre-treatment and the  
623 quantification of black carbon. *Quaternary Geochronology* 4, 140-147.

624 Bartlein, P.J., Harrison, S.P., Brewer, S., Connor, S., Davis, B.A.S., Gajewski, K., Guiot, J.,  
625 Harrison-Prentice, T.I., Henderson, A., Peyron, O. and Prentice, I.C., 2011. Pollen-  
626 based continental climate reconstructions at 6 and 21 ka: a global synthesis. *Climate*  
627 *Dynamics*, 37, 775-802.

628 Beringer, J., Hutley, L.B., Hacker, J.M., Neininger, B. 2011. Patterns and processes of  
629 carbon, water and energy cycles across northern Australian landscapes: from point to  
630 region. *Agricultural and Forest Meteorology* 151, 1409–1416.

631 Bird, M. I., Levchenko, V., Ascough, P. L., Meredith, W., Wurster, C. M., Williams, A.,  
632 Tilston, E.L., Snape, C.E. and Apperley, D. C., 2014. The efficiency of charcoal  
633 decontamination for radiocarbon dating by three pre-treatments—ABOX, ABA and  
634 hypy. *Quaternary Geochronology*, 22, 25-32.

635 Bird, M.I., Brand, M., Diefendorf, A.F., Haig, J.L., Hutley, L.B., Levchenko, V., Ridd, P.V.,  
636 et al., . 2019. Identifying the ‘savanna’ signature in lacustrine sediments in northern  
637 Australia. *Quaternary Science Reviews* 203, 233–247.

638 Blaauw, M., and Christen, J. A., 2011. Flexible paleoclimate age-depth models using an  
639 autoregressive gamma process. *Bayesian analysis* 6, 457-474.

640 Blonder, B., Enquist, B.J., Graae, B.J., Kattge, J., Maitner, B.S., Morueta-Holme, N.,  
641 Ordonez, A., et al., 2018. Late Quaternary climate legacies in contemporary plant  
642 functional composition. *Global Change Biology* 24, 4827–4840

643 Boland, D.J., Brooker, M.I.H., Chippendale, G.M., Hall, N., Hyland, B.P.M., Johnston, R.D.,  
644 Kleinig, D.A., McDonald, M.W., Turner, J.D. 2006. Forest trees of Australia. CSIRO  
645 Publishing, Melbourne.

646 Bornette, G., Puijalon, S., 2011. Response of aquatic plants to abiotic factors: a review.  
647 *Aquatic Sciences* 73, 1-14.

648 Brock, J., 1995. Remnant Vegetation Survey Darwin to Palmerston Region. A Report to  
649 Greening Australia, Darwin, Northern Territory.

650 Brock, J., 2001. Native plants of northern Australia. Reed New Holland, Sydney.

651 Bureau of Meteorology (BoM), 2019. Weather and Climate Data. Commonwealth of  
652 Australia. <http://www.bom.gov.au/climate/data/> (Accessed August 2019).

653 Burns, T., 1999. Subsistence and settlement patterns in the Darwin coastal region during the  
654 late Holocene: a preliminary report of archaeological research. *Australian Aboriginal*  
655 *Studies* 1, 59–69.

656 Charles, S., Petheram, C., Berthet, A., Browning, G., Hodgson, G., Wheeler, M., Yang, A., et  
657 al., 2016. Climate data and their characterisation for hydrological and agricultural  
658 scenario modelling across the Fitzroy, Darwin and Mitchell catchments: a technical  
659 report to the Australian Government from the CSIRO Northern Australia Water  
660 Resource Assessment, part of the National Water Infrastructure Development Fund:  
661 Water Resource Assessments. CSIRO, Australia.

662 Chen, W., Zhu, D., Ciais, P., Huang, C., Viovy, N., Kageyama, M., 2019. Response of  
663 vegetation cover to CO<sub>2</sub> and climate changes between last glacial maximum and pre-  
664 industrial period in a dynamic global vegetation model. *Quaternary Science Reviews*  
665 218, 293–305.

666 Clark, P.U., Dyke, A.S., Shakun, J.D., Carlson, A.E., Clark, J., Wohlfarth, B., Mitrovica, J.X.,  
667 Hostetler, S.W. and McCabe, A.M., 2009. The last glacial maximum. *Science*, 325,  
668 710-714.

669 Claussen, M., Selent, K., Brovkin, V., Raddatz, T., Gayler, V., 2013. Impact of CO<sub>2</sub> and  
670 climate on last glacial maximum vegetation—a factor separation. *Biogeosciences* 10,  
671 3593–3604.

672 Cleator, S., Harrison, S.P., Nichols, N., Prentice, I.C., Roulstone, I., 2019. A new multi-  
673 variable benchmark for last glacial maximum climate simulations. University of  
674 Reading. Dataset. DOI, 10 (1947.206).

675 Cook, G.D., Heerdegen, R.G., 2001. Spatial variation in the duration of the rainy season in  
676 monsoonal Australia. *International Journal of Climatology: A Journal of the Royal*  
677 *Meteorological Society* 21, 1723–1732.

678 Cook, G.D., Williams, R.J., Hutley, L.B., O'Grady, A.P. and Liedloff, A.C., 2002. Variation  
679 in vegetative water use in the savannas of the North Australian Tropical Transect.  
680 *Journal of Vegetation Science* 13, 413-418.

681 Cook, G.D., 1994. The fate of nutrients during fires in a tropical savanna. *Australian Journal*  
682 *of Ecology* 19, 359–365.

683 Dallmeyer, A., Claussen, M., Brovkin, V., 2019. Harmonising plant functional type  
684 distributions for evaluating earth system models. *Climate of the Past* 15, 335–366.

685 Denniston, R.F., Asmerom, Y., Polyak, V.J., Wanamaker Jr, A.D., Ummenhofer, C.C.,  
686 Humphreys, W.F., Cugley, J., Woods, D., Lucker, S., 2017. Decoupling of monsoon  
687 activity across the northern and southern Indo-Pacific during the late glacial.  
688 *Quaternary Science Reviews* 176, 101–105.

- 689 Fensham, R.J., Fairfax, R.J., Holman, J.E., 2002. Response of a rare herb (*Trioncinia*  
690 *retroflexa*) from semi-arid tropical grassland to occasional fire and grazing. *Austral*  
691 *Ecology* 27, 284–290.
- 692 Fitzsimmons, K.E., Miller, G.H., Spooner, N.A., Magee, J.W., 2012. Aridity in the monsoon  
693 zone as indicated by desert dune formation in the Gregory Lakes basin, northwestern  
694 Australia. *Australian Journal of Earth Sciences* 59, 469–478.
- 695 Ganopolski, A., Rahmstorf, S., Petoukhov, V., Claussen, M., 1998. Simulation of modern and  
696 glacial climates with a coupled global model of intermediate complexity. *Nature* 391,  
697 351–356.
- 698 Gavashelishvili, A., Tarkhnishvili, D., 2016. Biomes and human distribution during the last  
699 ice age. *Global Ecology and Biogeography* 25, 563–574.
- 700 Grimm, E.C., 1987. CONISS: a FORTRAN 77 program for stratigraphically constrained  
701 cluster analysis by the method of incremental sum of squares. *Computers and*  
702 *Geosciences* 13, 13–35
- 703 Grimm, E. C., 2004. Tilia graph v. 2.0.2. Illinois State Museum, Research and Collections  
704 Center.
- 705 Grubb, P.J., Metcalfe, D.J., 1996. Adaptation and inertia in the Australian tropical lowland  
706 rain-forest flora: contradictory trends in intergeneric and intrageneric comparisons of  
707 seed size in relation to light demand. *Functional Ecology* 10, 512–520.
- 708 Haberle, S.G., 2005. A 23,000-yr pollen record from Lake Euramoo, wet tropics of NE  
709 Queensland, Australia. *Quaternary Research* 64, 343–356.
- 710 Harrison, S.P., Prentice, C.I., 2003. Climate and CO<sub>2</sub> controls on global vegetation  
711 distribution at the last glacial maximum: analysis based on palaeovegetation data,  
712 biome modelling and palaeoclimate simulations. *Global Change Biology* 9, 983–1004.

713 Harrison, S.P., Bartlein, P.J., Izumi, K., Li, G., Annan, J., Hargreaves, J., Braconnot, P.,  
714 Kageyama, M., 2015. Evaluation of CMIP5 palaeo-simulations to improve climate  
715 projections. *Nature Climate Change*, 5, 735–743.

716 Hogg, A. G., Hua, Q., Blackwell, P. G., Niu, M., Buck, C. E., Guilderson, T. P., Heaton, T.J.,  
717 Palmer, J.G., Reimer, P.J., Reimer, R.W. and Turney, C. S., 2013. SHCal13 Southern  
718 Hemisphere calibration, 0–50,000 year cal BP. *Radiocarbon* 55, 1889-1903.

719 Hopcroft, P.O., Valdes, P.J., 2015. How well do simulated last glacial maximum tropical  
720 temperatures constrain equilibrium climate sensitivity? *Geophysical Research Letters*  
721 42, 5533–5539.

722 House, J.I., Archer, S., Breshears, D.D., Scholes, R.J., 2003. Conundrums in mixed woody–  
723 herbaceous plant systems. *Journal of Biogeography* 30, 1763–1777.

724 Hutley, L.B., Beringer, J., Isaac, P.R., Hacker, J.M., Cernusak, L.A., 2011. A sub-continental  
725 scale living laboratory: spatial patterns of savanna vegetation over a rainfall gradient  
726 in northern Australia. *Agricultural and Forest Meteorology* 151, 1417–1428.

727 Hutley L. B., Evans B. J., Beringer J., Cook G. D., Maier S. W., Razon, E., 2013. Impacts of  
728 an extreme cyclone event on landscape-scale savanna fire, productivity and  
729 greenhouse gas emissions. *Environmental Research Letters* 8, 1–12.

730 Hyland, B.P.M., Whiffin, T., and Zich, F.A., 2010. Australian Tropical Rainforest Plants.  
731 CSIRO Plant Industry and Centre for Australian National Biodiversity Research,  
732 Canberra.

733 Ishiwa, T., Yokoyama, Y., Okuno, J.I., Obrochta, S., Uehara, K., Ikehara, M., Miyairi, Y.,  
734 2019. A sea-level plateau preceding the Marine Isotope Stage 2 minima revealed by  
735 Australian sediments. *Scientific Reports* 9, 6449.



736 Jiang, D., Tian, Z., Lang, X., Kageyama, M., Ramstein, G., 2015. The concept of global  
737 monsoon applied to the last glacial maximum: a multi-model analysis. *Quaternary*  
738 *Science Reviews* 126, 126–139.

739 Liu, S., Jiang, D., Lang, X., 2018. A multi-model analysis of moisture changes during the last  
740 glacial maximum. *Quaternary Science Reviews* 191, 363–377.

741 Lu, Z., Miller, P.A., Zhang, Q., Wårlind, D., Nieradzik, L., Sjolte, J., Li, Q., Smith, B., 2019.  
742 Vegetation pattern and terrestrial carbon variation in past warm and cold climates.  
743 *Geophysical Research Letters* 8133–8143.

744 Calvo, M.M. and Prentice, I.C., 2015. Effects of fire and CO<sub>2</sub> on biogeography and primary  
745 production in glacial and modern climates. *New Phytologist* 208, 987–994.

746 Marshall, A.G., Lynch, A.H., 2008. The sensitivity of the Australian summer monsoon to  
747 climate forcing during the late Quaternary. *Journal of Geophysical Research:*  
748 *Atmospheres*, 113(D11).

749 McBeath, A.V., Wurster, C.M., Bird, M.I., 2015. Influence of feedstock properties and  
750 pyrolysis conditions on biochar carbon stability as determined by hydrogen pyrolysis.  
751 *Biomass and Bioenergy* 73, 155–173.

752 McFarlane, M.J., Ringrose, S., Giusti, L., Shaw, P.A., 1995. The origin and age of karstic  
753 depressions in the Darwin-Koolpinyah area of the Northern Territory of Australia. In:  
754 Brown (Ed.), *Geomorphology and Groundwater*. John Wiley and Sons Limited,  
755 Chichester, United Kingdom.

756 Meredith, W., Ascough, P. L., Bird, M. I., Large, D. J., Snape, C. E., Sun, Y., Tilston, E. L.  
757 2012. Assessment of hydrolysis as a method for the quantification of black  
758 carbon using standard reference materials. *Geochimica et Cosmochimica Acta* 97,  
759 131–147.

- 760 Moore, P., 2005. Plants of inland Australia. Reed New Holland, Sydney.
- 761 Moore C. E., Beringer J., Evans B., Hutley L. B., McHugh I., Tapper N. J., 2016. The  
762 contribution of trees and grasses to productivity of an Australian tropical savanna.  
763 *Biogeosciences* 13, 2387–2403.
- 764 Murphy B.P., Liedloff A.C., Cook ,G.D., 2015. Does fire limit tree biomass in Australian  
765 savannas? *International Journal of Wildland Fire* 24, 1–13.
- 766 Nano, C.E., Clarke, P.J., 2011. How do drought and fire influence the patterns of resprouting  
767 in Australian deserts? *Plant Ecology*, 212, 2095-2110.
- 768 Peel, M. C., Finlayson, B. L., and McMahon, T. A., 2007. Updated world map of the Köppen-  
769 Geiger climate classification. *Hydrology and earth system sciences discussions* 4, 439-  
770 473.
- 771 Pickett, E.J., Harrison, S.P., Hope, G., Harle, K., Dodson, J.R., Peter Kershaw, A., Colin  
772 Prentice, I., et al., 2004. Pollen-based reconstructions of biome distributions for  
773 Australia, Southeast Asia and the Pacific (SEAPAC region) at 0, 6000 and 18,000 <sup>14</sup>C  
774 yr BP. *Journal of Biogeography* 31, 1381–1444.
- 775 Prentice, I.C., Cramer, W., Harrison, S.P., Leemans, R., Monserud, R.A., Solomon, A.M.,  
776 1992. Special paper: a global biome model based on plant physiology and dominance,  
777 soil properties and climate. *Journal of Biogeography* 19, 117–134.
- 778 Prentice, I.C., Harrison, S.P., 2009. Ecosystem effects of CO<sub>2</sub> concentration: evidence from  
779 past climates. *Climate of the Past* 5, 297–307.
- 780 Prentice, I.C., Cleator, S.F., Huang, Y.H., Harrison, S.P. Roulstone, I., 2017. Reconstructing  
781 ice-age palaeoclimates: quantifying low-CO<sub>2</sub> effects on plants. *Global and Planetary*  
782 *Change* 149, 166–176.

783 Prior, L.D., 1997. Ecological Physiology of *Eucalyptus tetrodonta* (F. Muell.) and *Terminalia*  
784 *ferdinandiana* (Excell.) Saplings in the Northern Territory. Unpublished PhD thesis.  
785 Charles Darwin University, Northern Territory, Australi

786 Richards, A.E., Cook, G.D., Lynch, B.T., 2011. Optimal fire regimes for soil carbon storage  
787 in tropical savannas of northern Australia. *Ecosystems* 14, 503–518.

788 Rowe, C., Brand, M., Hutley, L.B., Wurster, C., Zwart, C., Levchenko, V., Bird, M., 2019a.  
789 Holocene savanna dynamics in the seasonal tropics of northern Australia. *Review of*  
790 *Palaeobotany and Palynology* 267, 17–31.

791 Rowe, C., Brand, M., Hutley, L.B., Zwart, C., Wurster, C., Levchenko, V., Bird, M., 2019b.  
792 Understanding Australian tropical savanna: environmental history from a pollen  
793 perspective. *Northern Territory Naturalist* 29, 2–11.

794 Russell-Smith, J., Setterfield, S.A., 2006. Monsoon rain forest seedling dynamics, northern  
795 Australia: contrasts with regeneration in eucalypt-dominated savannas. *Journal of*  
796 *Biogeography* 33, 1597–1614.

797 Russell-Smith, J. and Yates, C.P., 2007. Australian savanna fire regimes: context, scales,  
798 patchiness. *Fire ecology*, 3, pp.48-63.

799 Saiz, G., Wynn, J.G., Wurster, C.M., Goodrick, I., Nelson, P.N., Bird, M.I., 2015. Pyrogenic  
800 carbon from tropical savanna burning: production and stable isotope composition.  
801 *Biogeosciences* 12, 1849–1863.

802 Santamaría, L., 2002. Why most aquatic plants are widely distributed: dispersal, clonal  
803 growth and small-scale heterogeneity in a stressful environment. *Acta oecologica* 23,  
804 137–154.

805 Scott, K.A., Setterfield, S.A., Andersen, A.N., Douglas, M.M., 2009. Correlates of grass-  
806 species composition in a savanna woodland in northern Australia. *Australian Journal*  
807 *of Botany* 57, 10–17.

808 Scheiter, S., Higgins, S.I., Beringer, J., Hutley, L.B., 2015. Climate change and long-term fire  
809 management impacts on Australian savannas. *New Phytologist* 205, 1211–1226.

810 Scholes, R.J., Archer, S.R., 1997. Tree-grass interactions in savannas. *Annual Review of*  
811 *Ecological Systematics* 28, 517–544.

812 Schmitt, J., Schneider, R., Elsig, J., Leuenberger, D., Laurantou, A., Chappellaz, J., Kohler,  
813 P., et al., 2012. Carbon isotope constraints on the deglacial CO<sub>2</sub> rise from ice cores.  
814 *Science* 336, 711–714.

815 Schult, J., 2004. An Inventory of the Freshwater Lagoons in the Darwin Region. Report No.  
816 36/2004D, Water Monitoring Branch, Department of Infrastructure, Planning and  
817 Environment, Palmerston, Northern Territory.

818 Shakun, J.D., Carlson, A.E., 2010. A global perspective on last glacial maximum to Holocene  
819 climate change. *Quaternary Science Reviews* 29, 1801–1816.

820 Speck, N.H., Wright, R.L., Stewart, G.A., Fitzpatrick, E.A., Mabbutt, J.A., van de Graaf,  
821 R.H.M., 2010. General Report on Lands of the Tipperary Area, Northern Territory,  
822 1961. CSIRO Land Research Surveys, 13, 1–118.

823 Stevenson, J., Brockwell, S., Rowe, C., Proske, U., Shiner, J., 2015. The palaeo-  
824 environmental history of Big Willum Swamp, Weipa: an environmental context for  
825 the archaeological record. *Australian Archaeology* 80, 17–31.

826 Stuiver, M., and Polach, H. A., 1977. Reporting of C-14 data-Discussion. *Radiocarbon* 19,  
827 355-363.

- 828 Stuiver, M., and Reimer, P. J., 1993. Extended 14C data base and revised CALIB 3.0 14 C  
829 age calibration program. *Radiocarbon* 35, 215-230.
- 830 Thornhill, A.H., Hope, G.S., Craven, L.A., Crisp, M.D., 2012. Pollen morphology of the  
831 Myrtaceae. Part 1: tribes Eucalypteae, Lophostemoneae, Syncarpieae,  
832 Xanthostemoneae and subfamily Psiloxylloideae. *Australian Journal of Botany* 60, 65–  
833 199.
- 834 Vahdati, A.R., Weissmann, J.D., Timmermann, A., de León, M.S.P., Zollikofer, C.P., 2019.  
835 Drivers of late Pleistocene human survival and dispersal: an agent-based modeling  
836 and machine learning approach. *Quaternary Science Reviews* 221, 105867.
- 837 Van der Kaars, W.A., 1991. Palynology of eastern Indonesian marine piston-cores: a late  
838 Quaternary vegetational and climatic record for Australasia. *Palaeogeography,*  
839 *Palaeoclimatology, Palaeoecology* 85, 239–302.
- 840 Ward, J.K., Tissue, D.T., Thomas, R.B., Strain, B.R., 2001. Comparative responses of model  
841 C<sub>3</sub> and C<sub>4</sub> plants to drought in low and elevated CO<sub>2</sub>. *Global Change Biology* 5, 857–  
842 867.
- 843 Webb, L.J. and Tracey, J.G. 1994. The rainforests of northern Australia. In, Groves, R.H.  
844 (Ed.) Australian Vegetation. Cambridge University Press, Cambridge, UK, pp 87-130.
- 845 Weigelt, P., Steinbauer, M.J., Cabral, J.S., Kreft, H., 2016. Late Quaternary climate change  
846 shapes island biodiversity. *Nature* 532, 99–102.
- 847 Wells, S., 2001. Saltwater people: Larrakia stories from around Darwin. Larrakia Nation  
848 Aboriginal Corporation, Darwin, Northern Territory.
- 849 Whitlock, C., Larsen, C., 2002. Charcoal as a fire proxy. In: Smol, J.P., Birks, H.J.B., Last,  
850 W., Bradley, R.S., Alverson, K. (Eds.) Tracking Environmental Change Using Lake  
851 Sediments. Springer Publishing, Netherlands, pp. 75–97.

852 Williams, A.N., Ulm, S., Sapienza, T., Lewis, S., Turney, C.S., 2018. Sea-level change and  
853 demography during the last glacial termination and early Holocene across the  
854 Australian continent. *Quaternary Science Reviews* 182, 144–154.

855 Wurster, C.M., Lloyd, J., Goodrick, I., Saiz, G., Bird, M.I., 2012. Quantifying the abundance  
856 and stable isotope composition of pyrogenic carbon using hydrogen pyrolysis. *Rapid*  
857 *Communications in Mass Spectrometry* 26, 2690–2696.

858 Wurster, C.M., Saiz, G., Schneider, M.P.W., Schmidt, M.W.I., Bird, M.I., 2013. Quantifying  
859 pyrogenic carbon from thermosequences of wood and grass using hydrogen pyrolysis.  
860 *Organic Geochemistry* 62, 28–32.

861 Yan, M., Wang, B., Liu, J., Zhu, A., Ning, L., Cao, J., 2018. Understanding the Australian  
862 monsoon change during the last glacial maximum with a multi-model ensemble.  
863 *Climate of the Past* 14, 2037–2052.

864 Ye, J.S., Delgado-Baquerizo, M., Soliveres, S., Maestre, F.T., 2019. Multifunctionality debt  
865 in global drylands linked to past biome and climate. *Global Change Biology* 25,  
866 2152–2161.

867 Yokoyama, Y., Hirabayashi, S., Goto, K., Okuno, J.I., Sproson, A.D., Haraguchi, T.,  
868 Ratnayake, N. and Miyairi, Y., 2019. Holocene Indian Ocean sea level, Antarctic  
869 melting history and past Tsunami deposits inferred using sea level reconstructions  
870 from the Sri Lankan, Southeastern Indian and Maldivian coasts. *Quaternary Science*  
871 *Reviews*, 206, 150–161.

872 Zhu, D., Ciais, P., Chang, J., Krinner, G., Peng, S., Viovy, N., Peñuelas, J., Zimov, S., 2018.  
873 The large mean body size of mammalian herbivores explains the productivity paradox  
874 during the last glacial maximum. *Nature Ecology and Evolution* 2, 640–649.

875

ANSTO code	Submitter ID	Sample Type	Depth (cm)	pMC (%)	<sup>14</sup> C Age (yr BP)	1σ error (yrs BP)	Calibrated age 95% probability range (cal yr BP)	Calibrated age (median probability)
OZV442	GIR3 E45-50cm	hypy residue	455	19.9	12,970	80	15,154-17,517	15,692
OZV443	GIR3 F15-20cm	hypy residue	520	8.62	19,690	90	22,904-24,020	23,568
OZU820	GIR 3 F45cm	hypy residue	552	6.99	21,370	140	24,306-25,861	25,163
OZU821	GIR 3 G45cm	hypy residue	646	5.60	23,160	160	27,272-29,714	27,931

**Table 1.** <sup>14</sup>C radiocarbon AMS sample results used to develop the age model presented in Figure 2.

**Figure 1.** (color online) Location of Girraween Lagoon with current coastline mapped onto the landmass of Sahul, exposed by sea-level fall at the LGM. The outline of Sahul shown at a sea level equivalent to the 120 m isobath. Inset is a satellite image of the site and an image of the current dryland vegetation around the site.

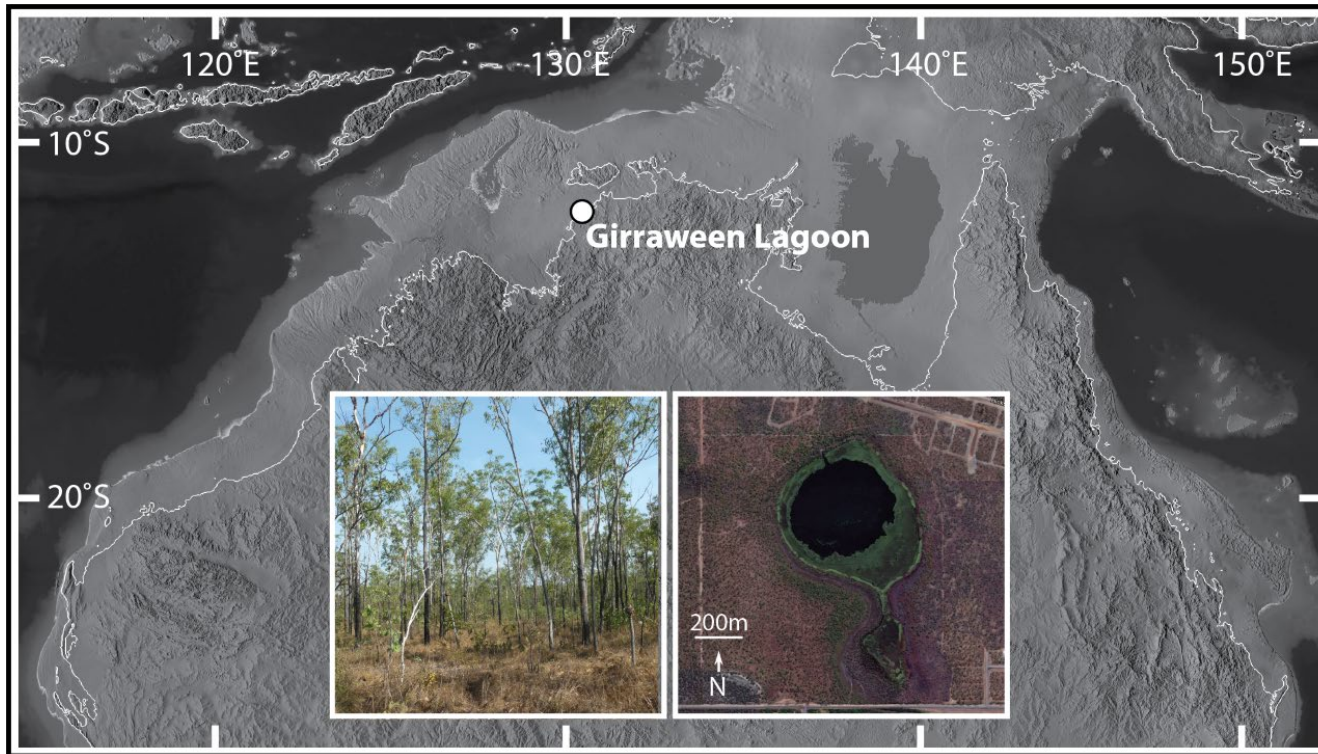




**Figure 2.** (color online) Age model developed for the interval of core under study. Inset is an optical image of the section from 478 to 595 cm, location of the samples for pollen analysis within the section and interval encompassing the LGM.

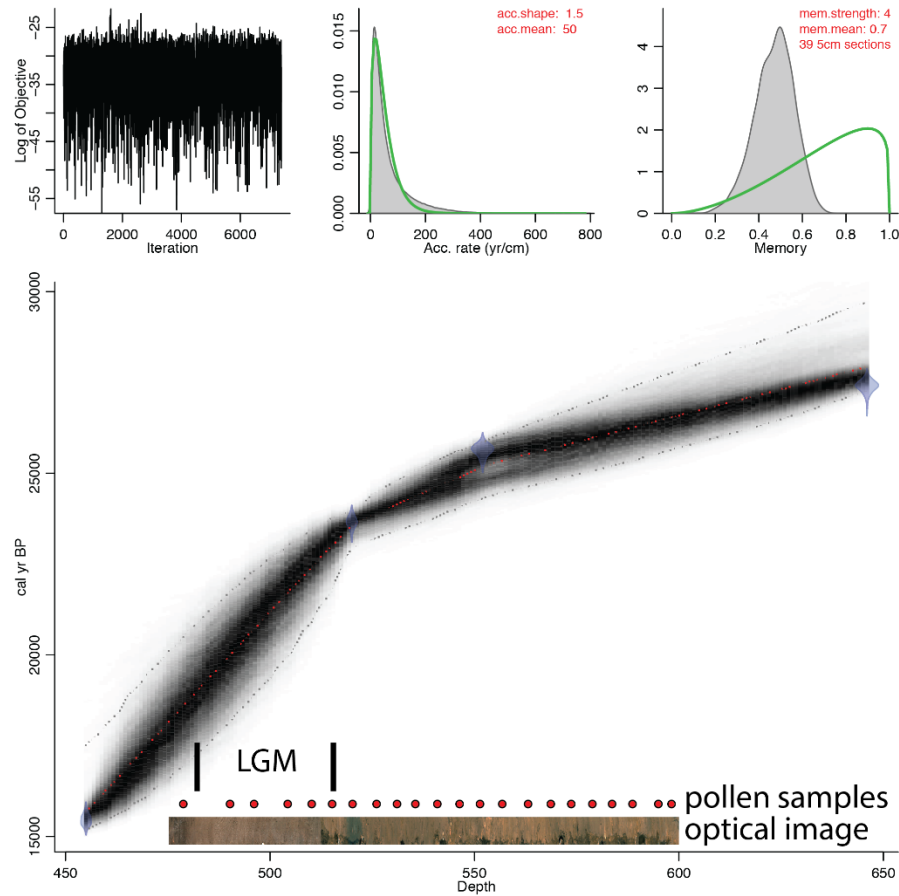
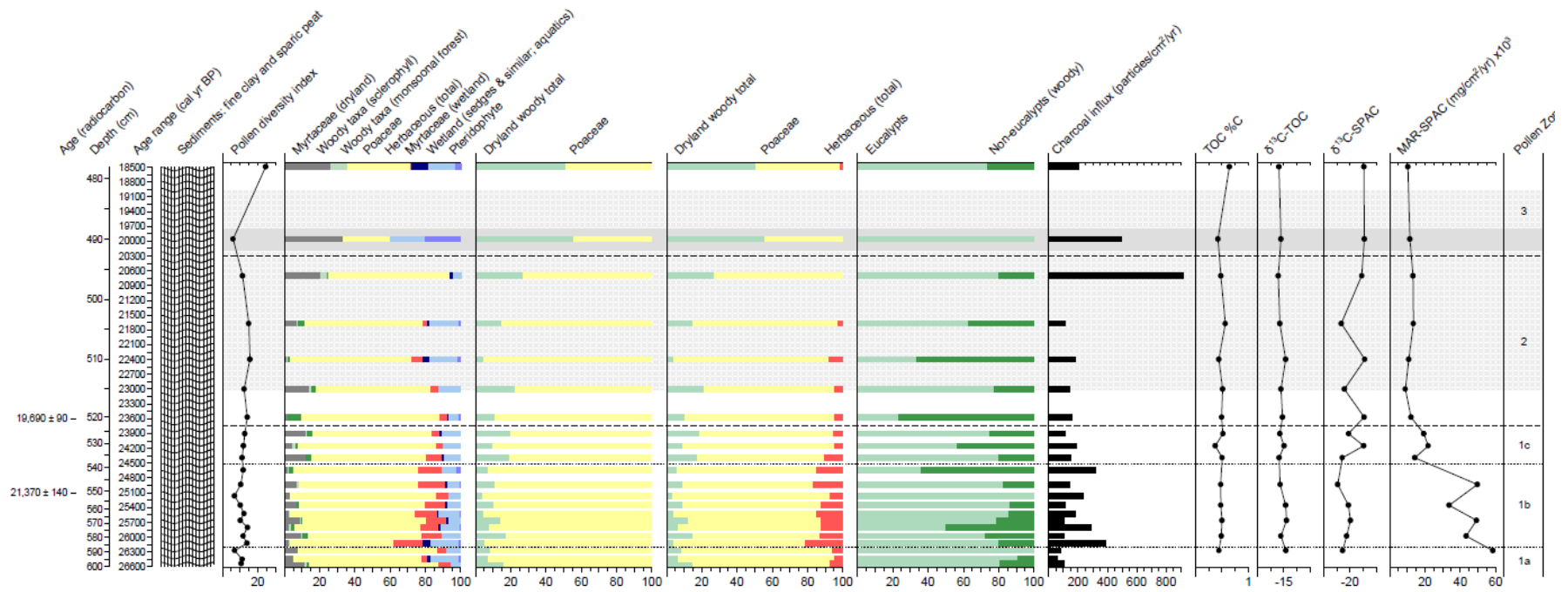
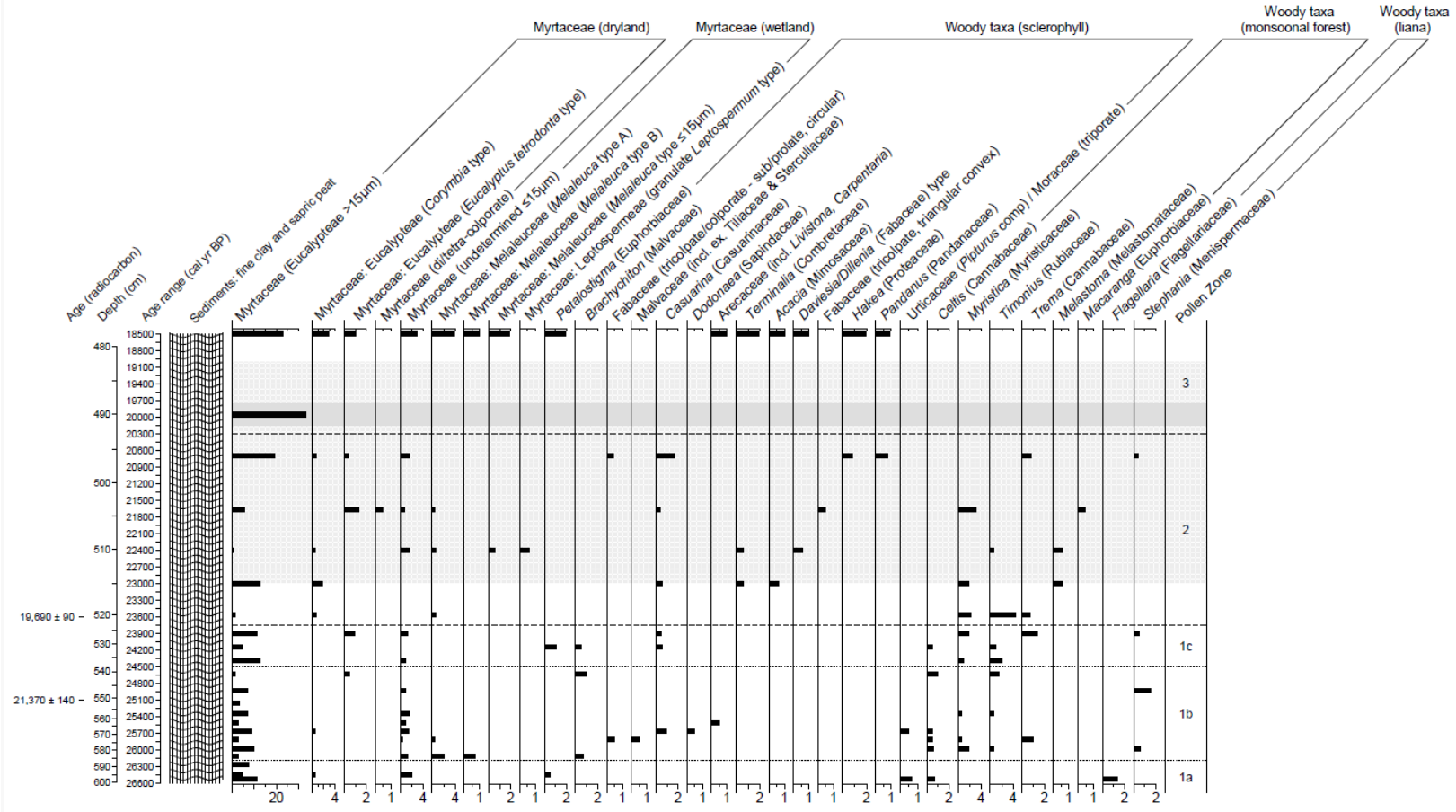


**Figure 3.** Girraween Lagoon percentage pollen diagram plotted against depth, stratigraphy, radiocarbon results, and calibrated age range. Data presentation divided into: a) pollen group summaries, microcharcoal and geochemical analyses. Note for the  $\delta^{13}\text{C}$  spectrum we consider -12.5‰ as the cut-off for 100%  $\text{C}_4$  grass biomass; b) woody pollen taxa; c) non-woody pollen taxa. The LGM has been highlighted in light grey, with poor pollen sample preservation outlined in darker grey. All percentages derived from total pollen sum including spores. The taxonomic level at which grain identification was most confident is that provided first. All data were plotted using TGView (Grimm, 2004) and pollen assemblages divided into zones based on the stratigraphically constrained classification undertaken by CONISS (Grimm, 1987; 2004). (For interpretation of the references to color in this figure legend, the reader is referred to the web version of this article.)

a) pollen group summaries, microcharcoal and geochemical analyses.



b) woody pollen taxa



c) non-woody pollen taxa.

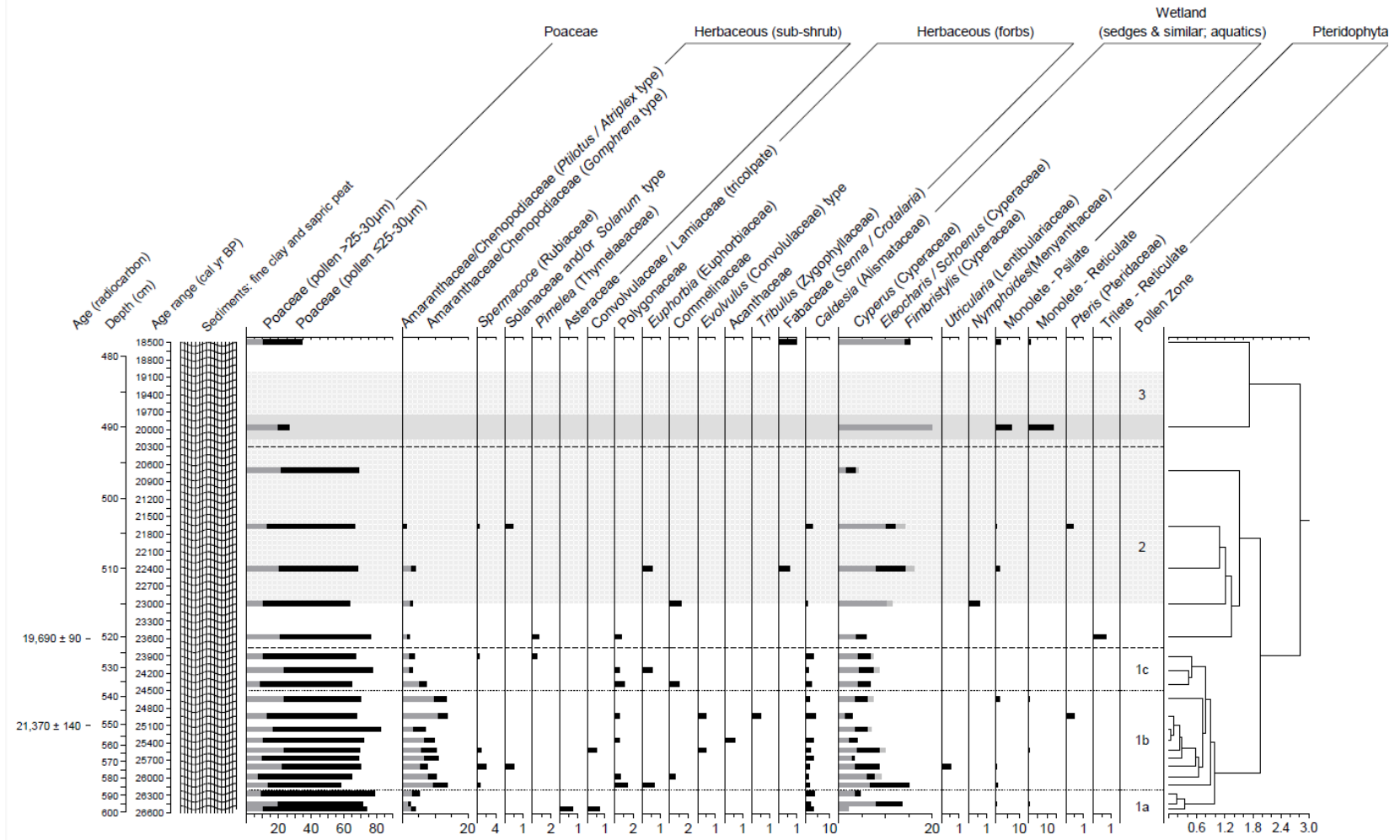


**Figure 4.** (color online) Representation of LGM vegetation based on the conclusion of decreased mean annual rainfall at Girraween Lagoon to within 700–1000 mm (annual precipitation derived from the general lower range for *Eucalyptus tetradonta*, and the precipitation implied by moving 300 km inland from Darwin today). Reduction in tree cover and stature, loss of woody-plant richness and expansion of grassland relative to current vegetation at the site: *left*, Girraween Lagoon, August 2018, and *right*, Jindare Station, September 2015, located within the Northern Territory's 1000 mm isohyet and illustrative of the upper range and conditions at Girraween during the last glacial phase.

